Numerical Investigation of the Effect of Ozone Addition on Detonation in the Two-dimensional RDE Chamber

Raimu Tanaka[1], Akiko Matsuo[1], Shima Eiji[1],
Hiroaki Watanabe[2], Akira Kawasaki[2], Ken Matsuoka[2], Jiro Kasahara[2]

[1]Department of Mechanical Engineering, Keio University
3-14-1 Hiyoshi, Kohoku, Yokohama, Kanagawa 223-8522, Japan

[2]Department of Aerospace Engineering, Nagoya University
Furo-cho, Chikusa, Nagoya, Aichi 464-8603, Japan

1 Introduction

The detonation is a type of premixed combustion in which combustion waves propagate at supersonic speed. In recent years, the applied research has been conducted to utilize the characteristics of the high pressure and speed of the detonation for engines. Typical examples of the detonation engine include Pulse Detonation Engine (PDE) and Rotating Detonation Engine (RDE). Since the detonation engines have higher theoretical thermal efficiency than the conventional rocket engines, and the compressor can be miniaturized [1], its application to kick motors is being considered. Especially, RDEs are attracting attention because it can obtain continuous thrust with a single ignition and the pressure gain due to the detonation leading shock waves [2]. However, the geometric [3] and thermodynamic constraints on the stable detonation propagation and the high heat load constrain the application of the detonation engines. To solve these problems, there is a lot of interest in the widening the detonation limits which would allow a broader use of fuels, lowered constraints on the oxidizer and more refined engine geometries.

Recently, the addition of radical species is attracting attention as a means of improving the stability of detonation and extending its limits. Previous studies on the combustion have shown that the significant reduction of the ignition delay, the expansion of the explosion limits [4] and the flame speed increase [5] via the addition of radical species to unburned mixtures. Especially, ozone (O_3) is attracting attention as a radical species. The oxidizing power of ozone is strong next to that of fluorine, and the high chemical reaction promoting effect can be expected. In addition, ozone can be cheaply and continuously produced via commercial ozone generators, making it suitable for use in practical applications. Crane et al. [6] confirmed that 3000 PPM ozone addition to hydrogen-oxygen (H_2-O_2) mixtures drastically reduce the average cell width with negligible change in the propagation velocity by the experimental cell measurement. Also, Shi et al. [7] showed that the ozone addition extends the detonation limits by moving the reaction mixture away from its geometric detonation limit, and as a results, trace amounts of ozone is expected to promote detonation propagation in geometric confined engines.

Correspondence to: raimu.t@keio.jp

When using ozone in detonation devices, knowledge about the effect of ozone on detonation and its mechanism is required. However, still few reports are available on the ozonated detonation. Especially, experiments and numerical analysis targeting a wider range of unburned mixture conditions and realistic systems are awaited. Hence, the objective of this study is to clarify the effect of ozone on detonation in RDE chamber by numerical analysis. In this paper, we focus on the circumferentially deployed pseudo-RDE chamber.

2 Numerical Aspects

The governing equations are the following two-dimensional compressible Euler equation and conservation law of chemical species.

$$\frac{\partial \mathbf{Q}}{\partial t} + \frac{\partial \mathbf{E}}{\partial x} + \frac{\partial \mathbf{F}}{\partial y} = \mathbf{S} \tag{1}$$

$$\mathbf{Q} = \begin{bmatrix} \rho \\ \rho u \\ \rho v \\ e \\ \rho_i \end{bmatrix}, \mathbf{E} = \begin{bmatrix} \rho u \\ p + \rho u^2 \\ \rho uv \\ (e+p)u \\ \rho_i u \end{bmatrix}, \mathbf{F} = \begin{bmatrix} \rho v \\ \rho vu \\ p + \rho v^2 \\ (e+p)v \\ \rho_i v \end{bmatrix}, \mathbf{S} = \begin{bmatrix} 0 \\ 0 \\ 0 \\ 0 \\ \omega_i \end{bmatrix}$$

Where t is the time, ρ is the density, u and v are the x and y direction velocity, e is the total energy, p is the pressure, ω is the formation reaction rate and subscript i represents the physical quantity for ith species. Also, to make the above equation system (1) closed-form, the thermally perfect ideal gas law:

$$p = \sum_i \rho_i R_i T \tag{2}$$

is used. Here, R is the gas constant and T is the temperature. AUSM-DV scheme [8] third-ordered by MUSCL is used for discretizing the convection term of Eq. (1). Also, three-step third-order TVD Runge-Kutta scheme [9] applied to the time integration of the fluid and Point Implicit method with 5 times inner iteration is applied to the time integration for the source term.

The analysis is performed on H_2-Air-O_3 mixtures, and the thermodynamic properties are calculated by NASA polynomials [10]. Chemical reaction models include the H_2-O_2 combustion reaction model

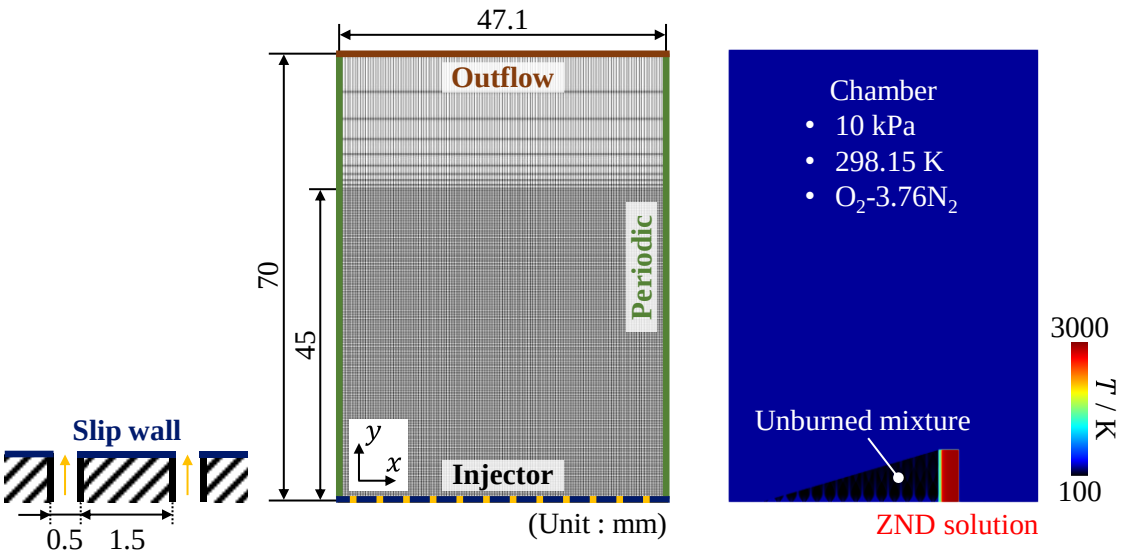

Figure 1: The two-dimensional computational structured mesh and initial condition setup of circumferencially deployed pseudo-RDE in this analysis.

proposed by Hong et al. [11], which considers the 20 elementary reactions including 9 species, and Princeton ozone sub-model [12], which considers the 11 elementary reactions including 20 species. Note that when introducing Princeton ozone sub-model, hydrocarbons were not dealt with in this analysis, so elementary reactions related to hydrocarbons were omitted. The chemical species considered in this analysis are 11 species: H_2, O_2, H, O, OH, H_2O, HO_2, H_2O_2, N_2, O_3 and O_2(SING), and the number of elementary reactions is 28. Here, O_2(SING) means singlet oxygen, which is a kind of the active oxygen.

The two-dimensional computational structured mesh and initial condition are shown in Fig. 1. The sizes of the calculation domain are determined with the reference to the cylindrical RDE used in the experiment by Yokoo et al. [13]. The mesh in domain around the bottom wall where detonation is propagated is refined. The bottom wall is an inflow boundary imitates injectors. The number of injectors is 24 and the total pressure and temperature are set to 1 MPa, 298.15 K respectively. And the composition of the gas to be injected is $2H_2$-O_2-$3.76N_2$, and the concentration of ozone is 0 or 3000 PPM. The outflow boundary is applied to the upper wall, which is fixed at 10 kPa when the flow is subsonic and extrapolated when the flow is supersonic. The second-order periodic boundary is used for the left and right wall. The initial condition consists of three regions: jet, ZND solution and others. First, a non-reaction calculation that considers only injection is conducted until the bottom pressure and temperature are almost in equilibrium. Next, the ZND solution at the pressure and temperature obtained from the above injection calculation (52.5 kPa, 145 K) is obtained. Finally, the jet is pasted in the triangular region and the ZND solution is pasted over 3 mm behind it. The minimum grid width is about 61.4 μm capturing the induction length obtained from the ZND calculation at around 5.7 pts. in the case without ozone and 1.3 pts. in the case with ozone. The total number of grid points is 615284.

3 Results and Discussion

Figure 2 shows that the temperature fields with (a) No O_3 and (b) 3000 PPM O_3 of the fully developed detonations. The relatively stable one detonation wave propagates from right to left over the entire calculation time regardless of ozone addition. However, there are some differences in the low temperature region showing unburned pockets between Figs. 2(a) and 2(b). Some unburned pockets can be seen above 15 mm in Fig. 2(a). But few such unburned pockets can be found in Fig. 2(b). Also, there

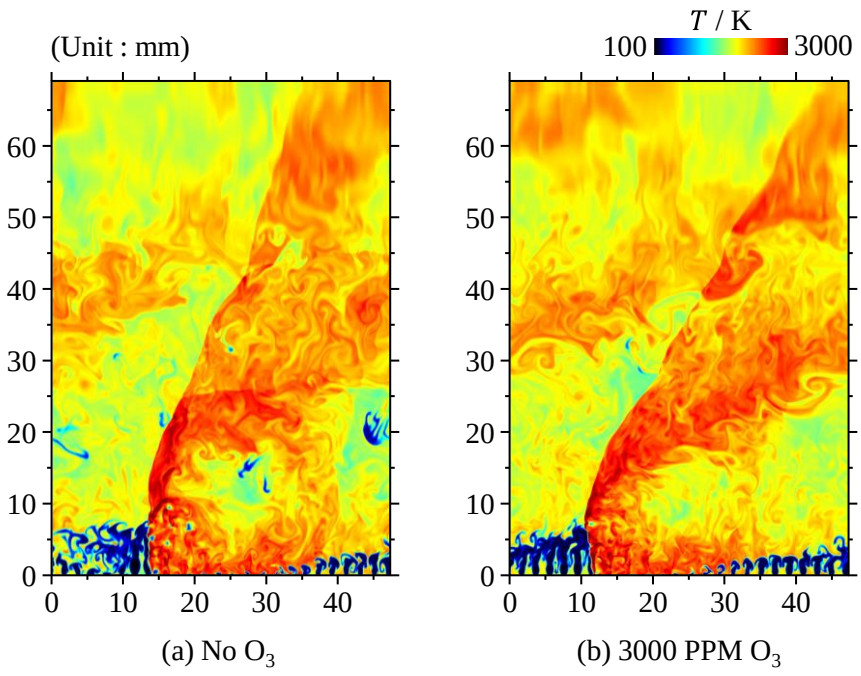

Figure 2: Qualitative comparison of temperature fields. (a) No ozone case. (b) 3000 PPM ozone case.

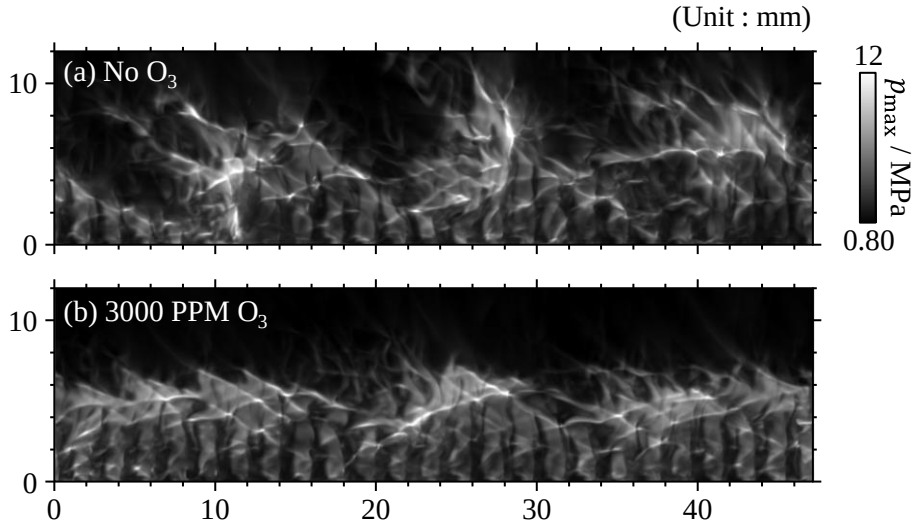

Figure 3: Cell pattern of the last lap. Here, $p_{\max}$ reepresents the maximam pressure. (a) No ozone case. (b) 3000 PPM ozone case.

Table 1: Average propagation velocity for each lap in the last three laps.

	Propagation velocity / m s^{-1}				
O_3 concentration / PPM	1st lap	2nd lap	3rd lap	Average	C-J state
0	1742	1527	1667	1645±89	1984
3000	1793	1776	1798	1798±9	1986

is a clear change in the angle of the oblique shock wave via the ozone addition. This indicates that the difference of the detonation propagation velocity between the two cases. The quantitative discussions on the propagation velocity will be described later.

To capture the characteristics of detonation in the RDE chamber, the cell patterns with (a) No O_3 and (b) 3000 PPM O_3 for the last lap are shown in Fig. 3. In Fig. 3(a), the high-pressure region can be seen in a relatively wide area from the bottom to a height of around 10 mm, and the cell pattern can hardly be observed. On the other hand, when ozone is added, the high-pressure region is within a height of around 7 mm, and cell patterns can be observed although they are irregular. This result indicates that the ozone addition can be expected to stabilize the flame in the RDE chamber. Unfortunately, the reduction of the cell size was not confirmed, as seen on the channel detonation in ref. [6].

Table 1 shows the perimeter average propagation velocity in each of the last three laps. Here, the propagation velocity was calculated using the average pressure time history from the bottom to 10 mm at the left end of the calculation domain. The C-J velocities in the table correspond to the one-dimensional steady detonation given as the initial condition. Table 1 indicates that ozone can improve the deficit of detonation propagation velocity in the RDE chamber. The velocity increase of approximately 8.7% was confirmed due to the 3000 PPM ozone addition. Hence, the velocity deficits based on C-J velocity has improved from approximately 17.1% to 9.9%. This velocity change could not be observed by the channel detonation analysis. In addition, the standard deviation that the variation of the velocity of each lap is reduced by ozone. This indicates that the detonation propagates more stably via the ozone addition.

Figure 4 shows that the spatiotemporal average profiles in the circumferential direction durring the last lap of (a) pressure, (b) temperature and (c) mole fraction of H_2. The upper figures are the overall view and lower figures are the enlarged view of the shaded region. The effect of ozone on the pressure is

small and almost the same profiles can be observed in Fig. 4(a). Also, we can clearly see the pressure peak near the bottom due to the detonation in Fig. 4(a). The position of the pressure peak is almost the same regardless of the ozone addition and it is a height of around 3 mm, and the behavior of the pressure drop after the peak is slightly different. The pressure decrease more rapidly and the foot of the peak become closer to the bottom from approximately 15 mm to 10 mm due to the 3000 PPM ozone. In Fig. 4(b), the temperature is relatively low near the bottom due to the low temperature unburned mixtures. And after combustion, the temperature is not change siginificantly until exhaust. The temperature profile is also similar regardless of the ozone addition, a temperature rise due to the ozone can be comfirmed in the Fig. 4(b). This is considered to be caused by the temperature increase of the burned gas and the desrease of the unburned pockets due to the ozone addition. The most of the H_2 is consumed within a height of 10 mm in both cases in Fig. 4(c). However, especially the region from a height of 10 mm to 30 mm, the mole fraction of H_2 in the case without ozone is about twice as big as that in the case with ozone. This means the decrease of the unburned pockets due to the ozone addition. These results indicate that ozone can be expected to help to the complete the combustion faster and improve the thermal efficiency.

4 Conclusions and Future Works

In this paper, the numerical analysis on the effects of ozone on detonation in the circumferentially deployed pseudo-RDE chamber is performed. And following conclusions are obtained.

- It is suggested that the ozone addition cause the high-pressure region to stay lower on the bottom. This suggests that combustion is completed closer to the bottom.
- Ozone has the potential to increase the detonation propagation velocity in the RDE chamber. In this study, 3000 PPM ozone provided the velocity increase of approximately 8.7%. This indicates that ozone may improve the velocity deficits and achieve more stable propagation.

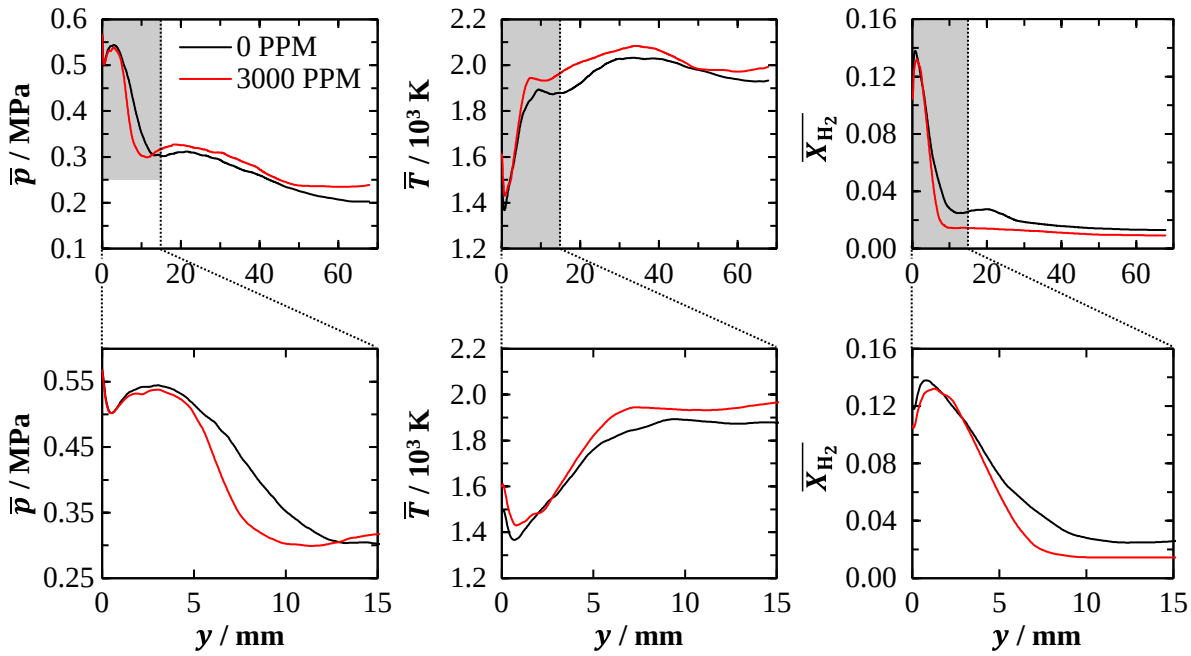

(a) Pressure (b) Temperature (c) Mole fraction of H_2

Figure 4: Spatiotemporal average profiles in the circumferential direction during the last lap. The lower figures are the enlarged view of the shaded regions in the upper figures.

What should be noted here is the low grid resolution. Although we were able to capture the trend of flow field changes due to the ozone addition, we plan to improve the quantitativeness and conduct more detailed studies by performing the analysis using fine grid.

References

[1] Kailasanath K. (2000). Review of propulsive applications of detonation waves. AIAA J. 38: 1698.

[2] Ma JZ., Luan M., Xia Z., Wang J., Zhang S., Yao S., Wang B. (2020). Recent progress, development trends, and consideration of continuous detonation engines. AIAA J. 58.

[3] Zhou R., Wu D., Wang J. (2016). Progress of continuously Rotating Detonation Engines. CJA. 29: 15.

[4] Liang W., Wang Y., Law CK. (2019). Role of ozone doping in the explosion limits of hydrogen-oxygen mixtures: multiplicity and catalyticity. Combust. Flame. 205: 7.

[5] Ji S., Wang H., Shu M., Tian G., Lan X., Li M., Li L., Cheng Y. (2019). Investigation of combustion enhancement by ozone in a constant-volume combustion bomb. Energy Fuel. 33: 9114.

[6] Crane J., Shi X., Singh AV., Tao YJ., Wang H. (2019). Isolating the effect of induction length on detonation structure: hydrogen-oxygen detonation promoted by ozone. Combust. Flame. 200: 44.

[7] Shi X., Crane J., Wang H. (2020). Detonation and its limit in small tubes with ozone sensitization. Proc. Combust. Inst. 38: 3547.

[8] Wada Y., Liou M. (1997). An accurate and robust flux splitting scheme for shock and contact discontinuities. J. Sci. Comput. 18:633.

[9] Gottieb S., Shu C. (1998). Total variation diminishing runge-kutta schemes. Math. Comput. 67: 73.

[10] Mcbride BJ., Gordon S., Reno MA. (1993). Coefficients for calculating thermodynamic and transport properties of individual species. NASA Tech. Memo. 4513 (NASA-TM-4513).

[11] Hong Z., Davidson DF., Hanson RK. (2011). An improved H_2/O_2 mechanism based on recent shock tube/laser absorption measurements. Combust. Flame. 158: 633.

[12] Hao Z., Xueliang Y., Yiguang J. (2016). Kinetic studies of ozone assisted low temperature oxidation of dimethyl ether in a flow reactor using molecular-beam mass spectrometry. Combust. Flame. 173: 187.

[13] Yokoo R., Goto K., Kasahara J., Athmanathan V., Braun J., Paniagua G., Meyer TR., Kawasaki A., Matsuoka K., Matsuo A., Funaki I., (2021). Experimental study of internal flow structures in cylindrical rotating detonation engines. Proc. Combust. Inst. 38: 3759.